# A novel time method for the simulation of the analog circuits driven by multi-tone signals

MIHAI IORDACHE, LUCIA DUMITRIU, CATALINA POPESCU

Electrical Engineering Department
"Politehnica" University of Bucharest
Spl. Independentei 313, Cod 06 0042, Bucharest
ROMANIA
Phone/Fax (+4021) 318 10 16 ,

*Key words*: Multiple time variables, Radio frequency analog circuit analysis.

The paper presents a new version of state variable method for circuit analysis with widely separated time scales. Widely-separated time scales appear in many electronic circuits, making traditional analysis difficult or impossible if the circuits are highly nonlinear. The key idea is to use multiple time variables, which enable signals with widely separated rates of variation to be represented efficiently. The differential algebraic equations (DAEs) describing the RF-IC circuits are transformed in multi-time partial differential equations (MPDEs). The time domain method presented in this paper is suitable for signals whose every component is influenced strong nonlinearities. Significant computation and memory result from using the new numerical technique. In order to solve MPDE we use the associated resistive discrete equivalent circuits (companion circuits) for the dynamic circuit elements.

## 1. Introduction

A very important step in the design of radio-frequency integrated circuits (RF-IC) is circuit simulation. A typical RF-IC application has carrier frequencies in the GHz-range with modulating signals in the kHz-range. Due to the broad signal spectrum (about six orders of magnitude) finding of the steady-state by the *brute-force method* is very time consuming [1, 2]. These signals are called *multirate signals*, and they contain "components" that vary at two or more widely separated rates. Such signals arise in various physical systems, as communication circuits (up/down-converters, automatic gain-control circuits), cycle-chopping and switched power converters, switched-capacitor filters, pulsewidth-modulation circuits etc. These systems are typically difficult to analyze using traditional numerical integration algorithms, such as those used in programs like SPICE [1]. The difficulty consists in the widely disparate rates: following fast-varying signal components long enough to obtain information about the slowly-varying ones is computationally expensive, and can also be inaccurate.

Many multirate signals, especially from circuits, can be represented efficiently as functions of two or more time variables, i.e. as *multivariate functions*. If a circuit is described with differential-algebraic equations (DAE), using multivariate functions for the unknowns leads naturally to a partial differential equation (PDE) form, which is called *Multirate Partial Differential Equation* (*MPDE*). If we apply time-domain numerical methods to solve the MPDE directly for the multivariate forms of the unknowns, we are able to analyze the combination of strong nonlinearities and multirate signals.

In the case of the lumped analog nonlinear circuits, because the numerical differentiation is a relatively inaccurate operation, we approximate the $q_k - v_k$ characteristic of each nonlinear capacitor and the $\varphi_k - i_k$ characteristic of each nonlinear inductor by piecewise-linear segments. In order to simplify the description of nonlinear resistors, their $v - i$ characteristics may be approximated by piecewise-linear continuous curves, or by new characteristics in which the nonlinearities are transferred to the sources, [7 - 9, 10 - 12]. Using the state equations (SEs) in partially symbolic form, we obtain a significant efficiency in circuit design and an improvement of the accuracy in the numerical calculations by considering as symbols only the parameters corresponding to the nonlinear circuit elements.

The State Equations (SE) and the output equation for lumped piecewise-linear nonlinear analogue circuits have the following form [11-13]:

$$\dot{\boldsymbol{x}} = \boldsymbol{A}\boldsymbol{x} + \boldsymbol{B}\boldsymbol{y} + \boldsymbol{B}_1\dot{\boldsymbol{y}}\,, \tag{1}$$

where: the matrices $\boldsymbol{A}$, $\boldsymbol{B}$ and $\boldsymbol{B}_1$ containg the incremental capacitances, the incremental inductances, the incremental rezistances and the incremental conductances corresponding to the nonlinear circuit elements, $\boldsymbol{x}(t)=\left[\boldsymbol{v}_{Ct}^{\mathrm{t}},\boldsymbol{i}_{Lc}^{\mathrm{t}}\right]^{\mathrm{t}}$ - is the state variable vector ($v_{Ct}$ - the tree branch capacitor voltages and $i_{Lc}$ - the link inductor currents) with $\boldsymbol{x}_0=\boldsymbol{x}(t_0)$ initial condition; $y=\left[\boldsymbol{e}^{\mathrm{t}},\boldsymbol{j}^{\mathrm{t}}\right]^{\mathrm{t}}$ - is the input vector, and the superscript "t" denotes the transpose.

If the analyzed circuit exhibits multirate behaviour, its variables can be represented efficiently using multiple time variables. If there are $p$ multivariate forms of change, $p$ time-scales are used. We denote the multivariate forms of $\boldsymbol{x}(t)$ and $\boldsymbol{y}(t)$ by $\hat{x}(t_1,...,t_p)$ and $\hat{y}(t_1,...,t_p)$.

The MPDE corresponding to (1) is:

$$\frac{\partial\hat{x}}{\partial t_1}+...+\frac{\partial\hat{x}}{\partial t_p}=A\hat{x}+B\hat{y}+B_1\left(\frac{\partial\hat{y}}{\partial t_1}+...+\frac{\partial\hat{y}}{\partial t_p}\right). \quad (2)$$

In [1] it is shown that there is a relation between the MPDE and the SEs of the circuit. According to the theorem 1 from [1] the solutions of the SEs are available on "diagonal" lines along the MPDE multivariate solutions.

Because the SEs are easy implemented in a program, we use these equations to obtain numerical solution of the MPDE. Replacing each capacitor and each inductor (magnetic coupled or not) by a discrete resistive circuit model associated with an implicit numerical integration algorithm, the transient analysis of nonlinear circuit can be reduced to the dc analysis of a sequence of equivalent nonlinear resistive circuits [4-7, 11, 12]. By using the backward differential formula of high order, the efficiency is achieved without compromising accuracy.

## 2. Method description

Considering the two-rate case, MPDE (2) becomes:

$$\frac{\partial\hat{\boldsymbol{x}}}{\partial t_1}+\frac{\partial\hat{\boldsymbol{x}}}{\partial t_2}=\boldsymbol{A}\hat{\boldsymbol{x}}+\boldsymbol{B}\hat{\boldsymbol{y}}+\boldsymbol{B}_1\left(\frac{\partial\hat{\boldsymbol{y}}}{\partial t_1}+\frac{\partial\hat{\boldsymbol{y}}}{\partial t_2}\right), \quad (3)$$

with the periodic boundary conditions (BCs) $\hat{x}(t_1+T_1,t_2+T_2)=\hat{x}(t_1,t_2)$. We consider a uniform grid $\bar{t}(i,j)\}$ of size $(p_2+1)\times(n_1+1)$ on the rectangle [0, $T_2$] x[0, $m_1T_1$] (Fig. 1). Here $\bar{t}(i,j)=(t_{2_i},t_{1_j})$, $t_{2_i}=(i-1)h_2p_2=(i-1)T_2$ (at each integration step $h_1$ we perform $p_2$ integrations with size step $h_2$), $t_{1_j}=(j-1)h_1$, $1\le i\le p_2+1,\ 1\le j\le n_1+1$, $h_1=m_1T_1/n_1=T_1/p_1$ and $h_2=T_2/p_2$ are the grid spaces in the directions $t_1$ and $t_2$ respectively. We consider that the slow components of $y(t)$ and $\boldsymbol{x}(t)$ depend on $t_1$ and the fast components of $y(t)$ and $\boldsymbol{x}(t)$ depend on $t_2$.

In order to integrate the state equation (15) we use the backward-differentiation formula (BDF) [22], which approximates to within prescribed accuracy the present value $\dot{x}(t_{n+1})$ of the time derivative of $x(t_{n+1})$ in terms of $x_{n+1}$ and $p$ past values $x_n,x_{n-1},...,x_{n-p+1}$:

$$\dot{x}_{n+1}=\frac{1}{h}\sum_{k=0}^{p}a_kx_{n+1-k}=\frac{1}{h}\left(x_{\_n}-x_{\_o}\right), \quad (4)$$

where: $a_0,a_1,...,a_p$ are constants, $h=t_{n+1}-t_n$ is the present step size, $x_{\_n}=a_0x_{n+1}$ is the new value of $x$,

We can also use the following numerical implicit integration algorithms: the trapezoidal algorithm and the Gear's algorithm.

For the first periods $T_1$ and $T_2$ (corresponding to the grid of size $(p_2+1)\times(p_1+1)$), we assume that the BCs are: $\hat{\boldsymbol{x}}(i,1)=0.0;\ i=\overline{1,p_2+1}$, and $\hat{\boldsymbol{x}}(1,j)=0.0;\ j=1,2$ and $\hat{\boldsymbol{x}}(1,j+1)=\hat{\boldsymbol{x}}(p_2+1,j);\ j=\overline{2,p_1+1}$, on the column $t_1=0$, and on the row $t_2=0$ respectively. We start the integration process on the column 2 from the point $\bar{t}(2,2)=(t_{2_2},t_{1_2})$, with $t_{2_2}=h_2,t_{1_2}=h_1$ on the column 2 (in respect of the fast time $t_2$) from the row 2 to the row $p_2$+1 and so on till we arrive in the point $\bar{t}(p_2+1,2)=(t_{2_{p2+1}},t_{1_1})$, with $t_{2_{p2+1}}=p_2h_2=T_2,t_{1_2}=h_1$. After that, we integrate one time step $h_1$ in respect of the slow time $t_1$ (in this point we assign to $\hat{x}(1,3)$ the value of $\hat{x}(p_2+1,2)$) and then we again start the integration process on the column 3 (in respect of the fast time $t_2$) from the row 2 to the row $p_2$+1 and so on till we arrive in the point $\bar{t}(p_2+1, p_1+1) = \left(t_{2_{p_2+1}}, t_{1_{p_1+1}}\right)$, with $t_{2_{p_2+1}} = p_1 h_2 p_2 = p_1 T_2$ (at each integration step $h_1$ we perform $p_2$ integrations with size step $h_2$) and $t_{1_{p_1+1}} = p_1 h_1 = T_1$.

**Remark 1.** Before of the passing to the integration for the next periods $T_1$ and $T_2$ (corresponding to the grid of size $(p_2+1)\times(p_1+1)$), which it starts from the point $\bar{t}(2, p_1+1) = \left(t_{2_2}, t_{1_{p_1+1}}\right)$, with $t_{2_2} = p_1 p_2 h_2 + h_2 = p_1 T_2 + h_2$ and $t_{1_{p_1+1}} = (p_1+1)h_1 = T_1 + h_1$, we must consider the following boundary conditions: $\hat{x}(1, p_1+2) = \hat{x}(p_2+1, p_1+1)$, and $\hat{x}(1, p_1+j+1) = \hat{x}(p_2+1, p_1+j)$, $j = \overline{2, p_1+1}$ on the row $t_2 = 0$ and $\hat{x}(i, p_1+1)$, $i = \overline{2, p_2+1}$ on the column $t_1 = T_1$. After that, it is performed an integration with the integration step $h_1$ in respect of the slow time $t_1$ from the point $\bar{t}(p_2+1, p_1+1)$ to the point $\bar{t}(2, p_1+2)$ (in this point we assign to $\hat{x}(1, p_1+2)$ the value of $\hat{x}(p_2+1, p_1+1)$) (see Fig. 1).

Proceeding in this way for the other periods $T_1$ and $T_2$ we shall integrate the MPDE on the whole uniform grid of size $(p_2+1)\times(n_1+1)$, when we arrived in the point $\bar{t}(p_2+1, n_1+1) = \left(t_{2_{p_2+1}}, t_{1_{n_1+1}}\right)$, with $t_{2_{p_2+1}} = p_2 h_2 m_1 p_1 = m_1 p_1 T_2 = n_1 T_2$ (because at each integration step $h_1$ we perform $p_2$ integrations with size step $h_2$), and $t_{1_{n_1+1}} = n_1 h_1 = m_1 p_1 h_1 = m_1 T_1$.

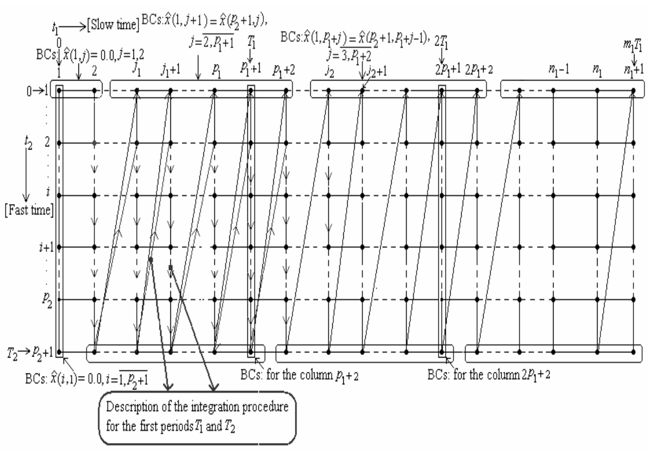


Fig. 1. A uniform grid $\{\bar{t}(i, j)\}$ of size $(p_2+1)\times(n_1+1)$.

At each time moment $\bar{t}(i, j)$ we have to solve a nonlinear algebraic equation system. For this, we can use the Newton-Raphson algorithm or other efficient numerical iteration algorithms [1-7, 13].

The discrete resistive circuit equations, associated with the BDF of the first order ($a_0 = 1$ and $a_1 = -1$) when the characteristics of the nonlinear elements are approximated by piecewise-linear continuous curves, at $\bar{t}(i, j)$ (with,. $t_{2i} = (i-1)h_2 + (j-1)T_2$ and $t_{1j} = (j-1)h_1$) (at each integration step $h_1$ we perform $p_2$ integrations with size step $h_2$), and at the $(k+1)^{\text{th}}$ iteration of the Newton-Raphson algorithm, corresponding to the state equations (4), have the following form:

$$\frac{1}{h_1}\left(\boldsymbol{x}_{\_n} - \boldsymbol{x}_{\_o}\right) + \frac{1}{h_2}\left(\boldsymbol{x}_{\_n} - \boldsymbol{x}_{\_o}\right) = \boldsymbol{A}\boldsymbol{x}_{\_n} + \\ + \boldsymbol{B}\boldsymbol{y}_{\_n} + \boldsymbol{B}_1\left[\frac{1}{h_1}\left(\boldsymbol{y}_{\_n} - \boldsymbol{y}_{\_o}\right) + \frac{1}{h_2}\left(\boldsymbol{y}_{\_n} - \boldsymbol{y}_{\_o}\right)\right] \tag{5}$$

where: $x_{\_n} = x(i, j)$ is the new value of state vector $\boldsymbol{x}$ at $\bar{t}(i, j)$, $\boldsymbol{x}_{\_o1} = \boldsymbol{x}(i, j-1)$ ($\boldsymbol{x}_{\_o2} = \boldsymbol{x}(i-1, j)$) is the "old" value of state vector $\boldsymbol{x}$. at the moment $\bar{t}(i, j-1)$ (at the moment $\bar{t}(i-1, j)$), $\boldsymbol{y}_{\_n} = \boldsymbol{y}(i, j)$ is the new value of input vector $\boldsymbol{y}$ at $\bar{t}(i, j)$, $\boldsymbol{y}_{\_o1} = \boldsymbol{y}(i, j-1)$ ($\boldsymbol{y}_{\_o2} = \boldsymbol{y}(i-1, j)$) is the "old" value of input vector $\boldsymbol{y}$ at the moment $\bar{t}(i, j-1)$ (at the moment $\bar{t}(i-1, j)$). The vectors: $\boldsymbol{y}(i, j)$, $\boldsymbol{y}(i, j-1)$ and $\boldsymbol{y}(i-1, j)$ represent the contributions of the excitation sources (independent current and voltage sources), of the sources corresponding to the approximations of nonlinear resistors and the initial values of the inductor currents and of the capacitor voltages which are determined from previous time steps $\bar{t}(i-1, j)$ of the slow time $t_1$, and $\bar{t}(i, j-1)$ of the fast time $t_2$. The subscripts $(i, j)$, $(i, j-1)$, $(i, 1)$ and $(i-1, 1)$ represent the time moments.

The structure of the equations (5) leads to the elimination of the state variable that appears in the least number of state equations. Elimination procedure is equivalent to substituting the variable involving in the smallest number of equations and removing the equation involving the smallest number of variables (one of which is the variable to be eliminated) in the state equations (5). According to this rule, we select the state equations corresponding to the eliminated state variables and introducing them in the remained state equations, we obtain the state equations in the normal form for the remained state variables. These state equations have as symbols the old values of all state variables and time step size. The remained state equations can easy be integrated to obtain the circuit response. With this approach we obtain important savings in computing time and memory.

The algorithm for large-scale circuit decomposition, and the method to systematically formulate the state equations in partially symbolic normal-form for linear and/or nonlinear time-invariant large-scale analog circuits with excess elements, was implemented in **SYSEG** – **SY**mbolic **S**tate **E**quation **G**eneration- program [11].

## 3. Examples

In Fig. 2 is shown the equivalent circuit for the TV video-frequency circuit. The voltage-controlled nonlinear resistor $R_{13}$ is modeled by an equivalent scheme corresponding to the approximation of the *v-i* characteristic by a continuos piecewise linear curve:

| | | | | |
|---|---|---|---|---|
| $U_{13}$ [V] | -1000.0 | 0.0 | 0.1 | 100.0 |
| $I_{13}$ [mA] | -1.0e-15 | 0.0 | 10.0 | 10000.0 |

The state vector has the following strucure:

***X*** = [UC5, UC6, UC7, UC8, UC9, IL22, IL23, IL24, UC2, UC4, UC3]$^t$ (6)

The eliminated state variables are:

***El_st_vars*** = [UC5, IL22, IL23, IL24, UC9, UC4]$^t$ (7)

The remained state equations in partially-symbolic normal form, when we consider as symbols the input vector, the "old" value of state variables and the associated parameters to the nonlinear circuit elements, (the full symbolic form can be obtained, but it is a very large expression) of the circuit in Fig. 2, have the form:

```
Rem_st_eqs:={1.500*UC8_n--
.5000*UC8_o1-1.000*UC8_o2=
=.2859e-1*UC5_o2+.1624e-4*e1+
.1429e-1*UC5_o1++.4639e-
3*IL22_o1+.9278e*IL22_o2+
+.4290e-1*UC6_n-.2893e-1*UC9_o2+
+.2706e-3*IL23_o2+.1353e-3*IL24_o1
+.2706e-3*IL24_o2-.1624e-4*UC2_n+
+.2639e-3*UC4_o1+.5280e-
3*UC4_o2+.2593e-4*UC3_n-.4505e-
1*UC8_n-.8078e-5*UC7_n+.1353e-
3*IL23_o1-.1446e-1*UC9_o1 ;
1.500*UC3_n-.5000*UC3_o1-
1.000*UC3_o2=-.2131e-1*UC5_o2
+.1268e-2*e1-.1066e-1*UC5_o1-
.1138e-1*IL22_o1-.2276e-1*IL22_o2-
.3249e-1*UC6_n+.1245e-1*UC9_o2-
.6638e-2*IL23_o2-.3319e-2*IL24_o1-
.6638e-2*IL24_o2-.1268e-2*UC2_n+
+.4683e-2*UC4_o1+.9367e-2*UC4_o2
-.2303e-2*UC3_n+.1879e-1*UC8_n+
.+.1981e-3*UC7_n-.3319e-*IL23_o1+
+.6220e-2*UC9_o1 ;
1.500*UC6_n-.5000*UC6_o1-              (8)
1.000*UC6_o2=-.1204e-1*UC5_o2
+.1540e-3*e1-.6017e-2*UC5_o1+
.4401e-2*IL22_o1+.8804e-2*IL22_o2-
.2003e-1*UC6_n+.6654e-2*UC9_o2-
.2520e-1*IL23_o2-.1261e-1*IL24_o1-
-.2520e-1*IL24_o2-.1540e-3*UC2_n+
+.2505e-2*UC4_o1+.5011e-2*UC4_o2
+.2460e-3*UC3_n+.1006e-1*UC8_n
+.7525e-3*UC7_n-.1261e-1*IL23_o1
+.3327e-2*UC9_o1 ;
1.500*UC7_n-.5000*UC7_o1-
1.000*UC7_o2=-.3074e-
1*UC7_n+.1960e-1*IL23_o1+.3922e-
1*IL23_o2+.1170e-2*UC6_n,
1.500*UC2_n-.5000*UC2_o1-
1.000*UC2_o2 = .8335e-2*e1-.8335e-
2*UC3_n-.8335e-2*UC2_n-
-.5000/Rdu13*UC2_n-.5000*Ij14};
```

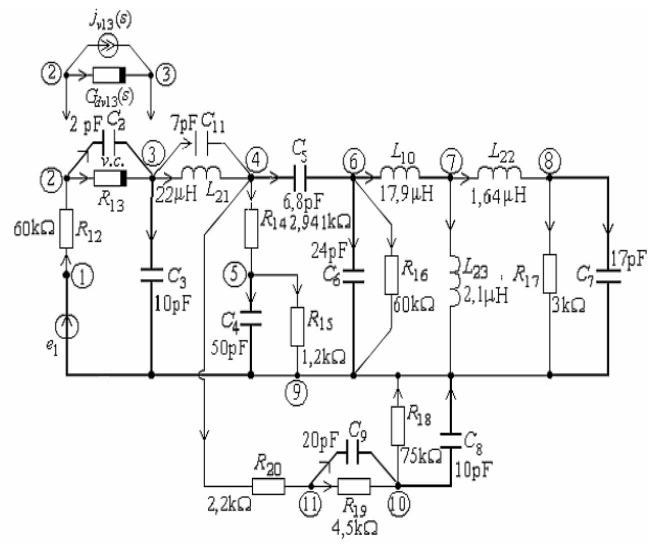


Fig. 2. Diagram of the TV video-frequency circuit

If we assume that the input signal $e_1(t)$ has the following expression:

$$e_1(t) = (1.0 + 0.9\sin(2\pi f_{MA} t))\sin(2\pi f_0)\, V,\ f_{MA} = 4MHz,$$

The bi-variate excitations have the expressions:

$$\hat{e}_1(t_1, t_2) = (1.0 + 0.9\sin(2\pi f_{MA} t_1))\sin(2\pi f_0 t_2)\, V,$$

$$f_{MA} = 4MHz, \quad f_0 = 400MHz$$

and was plotted in Fig. 3.

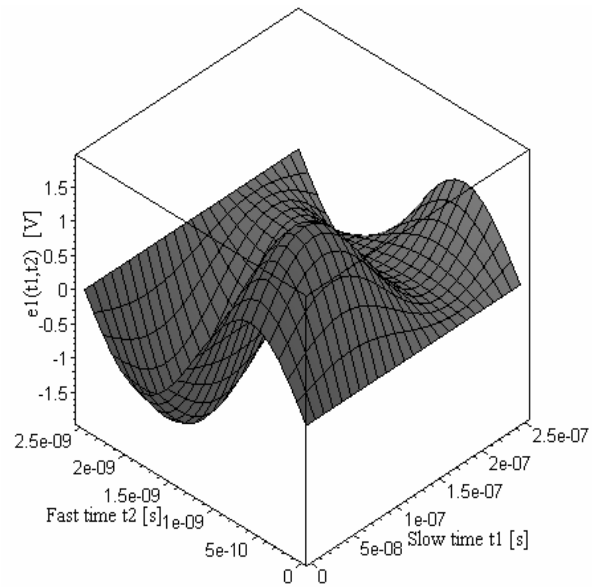


Fig.3. The bi-variate excitation $e_1(t_1, t_2)$

Using the method presented in Section 2 the variations of the capacitor voltages $v_{C2}$, $v_{C8}$ and the inductor current $i_{L21}$, in respect to the time, are shown in Figures4, 6, and 8, respectively, in a representation with two-time variables and in Figures 7, 8, and 9, respectively, in a one-time variable representation.

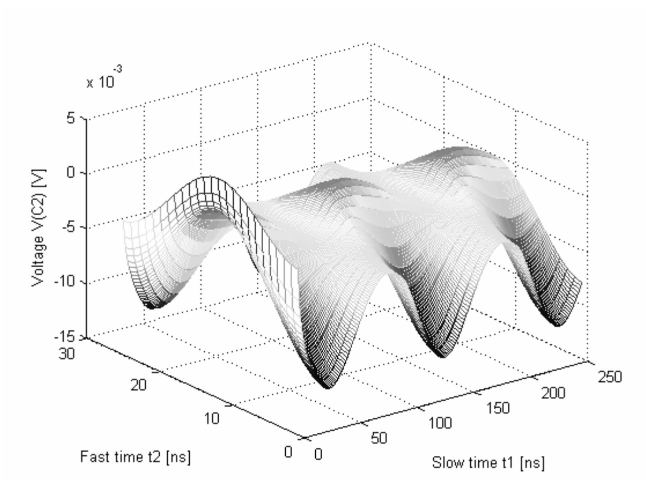


Fig. 4. Two-time variation of the output voltage $v_{C2}$.

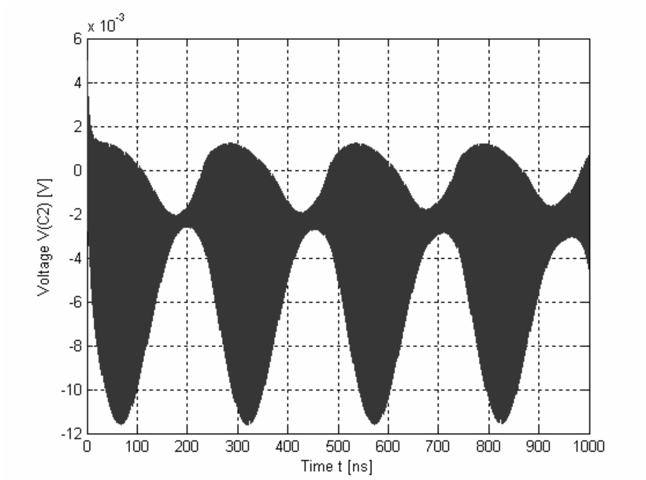


Fig.5.One-time variation of the output voltage $v_{C2}$.

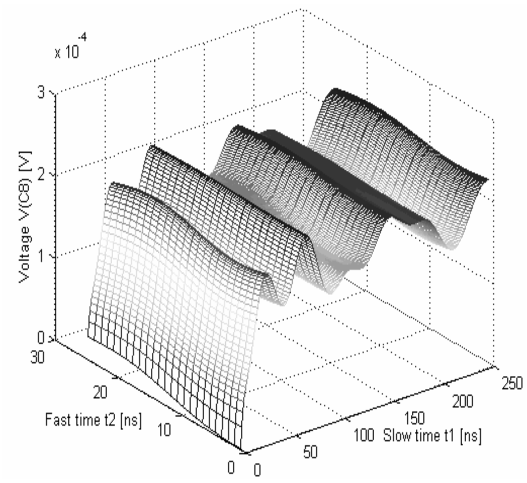


Fig. 6. Two-time variation of the output voltage $v_{C8}$.

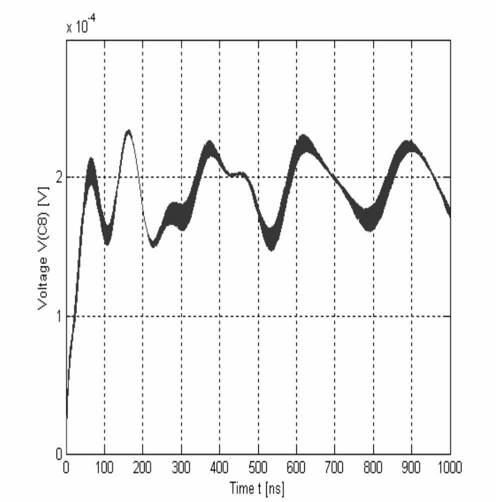


Fig.7.One-time variation of the output voltage $v_{C8}$.

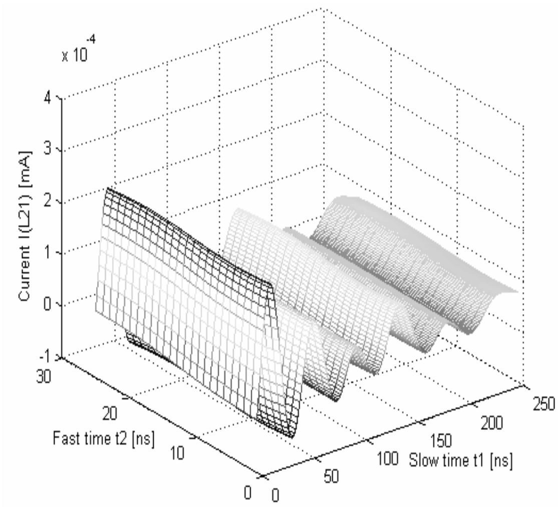


Fig. 8. Two-time variation of the output voltagei$_{L21}$.

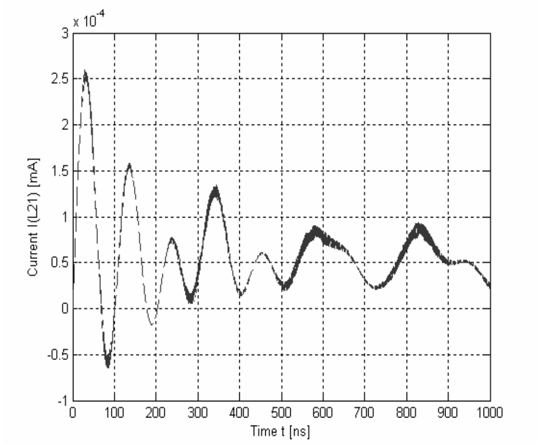


Fig. 9. One-time variation of the output voltage $i_{L21}$.

Consider the diode mixer shown in Fig. 10.
The input single-time singles have the following expressions:

$$v_1(t) = 0.01\sin\left(2\pi 9.95 10^9 t\right)\mathrm{V},\ v_2(t) = 2\sin\left(2\pi 10^{10} t\right)\mathrm{V}.$$

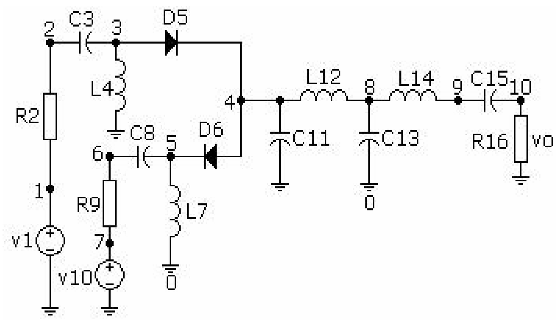


Fig.10. Diode mixer.

Using the method presented in Section II the variation output voltage $u_{C6}$ with respect to time is shown in Fig. 11.

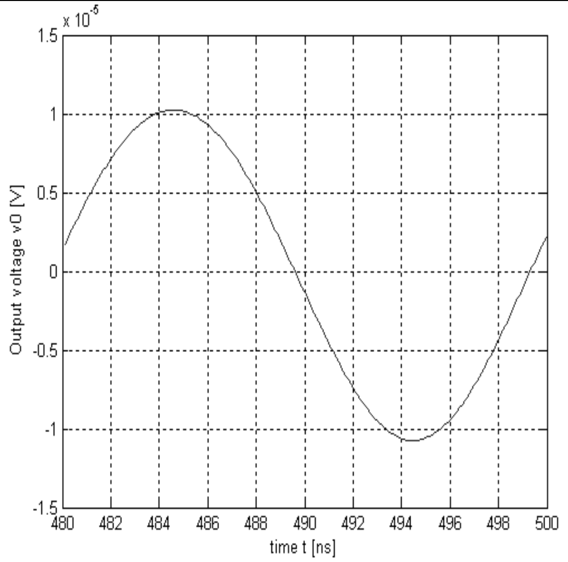

Single-time solution.

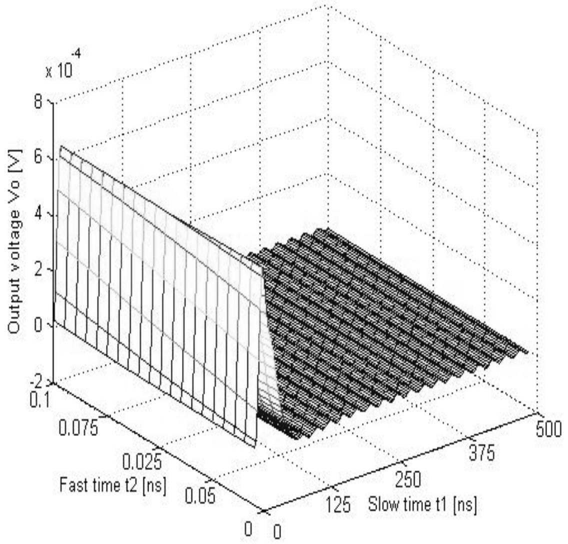

Muti-time solution.

Fig. 11. Variation of the output voltage $v_o$.

Simulation with one time variable has been performed using 20000 samples per period $T_2$ = 20 ns, CPU time was of 100 times greater than in the case when the simulation has been performed with two time variables (when we used 200 samples per period $T_2$ = 20 ns, and 20 samples per period $T_2$ = 0.1 ns). The output filter has the central frequency equal to $50.10^6$ Hz.

## 4. Conclusion

An efficient numerical approach for analyzing strongly nonlinear multirate circuits has been presented. The procedure uses multiple time variables to describe multirate behaviour, leading to a PDE called the MPDE. Applying appropriate BCs to this MPDE and using the state equations lead to quasi-periodic and envelope-modulated solutions. By using the backward differential formula of high order, the efficiency is achieved without compromising accuracy. Presenting the results in three-dimensional form is useful for visualizing waveforms with widely separated time scales (as in the case of RF-IC). The new technique can solve a variety of circuits that are hard to simulate with a mix of strong and weak nonlinearities.

Acknowledgment
This research is financed from CNCSIS grant – C38.

*References*

1. J. Roychowdhury, *Analyzing Circuits with Widely Separated Time Scales Using Numerical PDE Methods*, IEEE Trans. on CAS – I, **48**, *5*, pp. 578-594 (2001).
2. Fl. Constantinescu, Miruna Nitescu, *A new multi-rate method for analysis of RF-IC circuits*, Proc. of the International Symposium on Signals, Circuits and Systems, SCS'03, Iasi, Romania, July, 10-11, pp. 91-94 (2001).
3. H. G. Brachtendorf, G. Welsch, R. L. Laur, *A novel time-frequency method for the simulation of the steady state of circuits driven by multi-tone signals*, Proc. on ISCAS, June 9-12, Hong Kong, pp.1508-1511(1997).
4. C.W. Ho, A. E. Ruehli, P. A. Brennan, *The modified nodal approach to network analysis*, IEEE, Trans., CAS, **22**, *5*, pp. 504-509 (1975).
5. A. E. Schwarz, C*omputer-aided design of microelectronic circuits and systems*, Academic Press, London, 1987.
6. L. O. Chua, and P. M. Lin, *Computer-Aided Analysis of Electronic Circuits: Algorithms and Computational Techniques*, Englewood Cliffs, NJ: Prentice-Hall, 1975.
7. A. Ushida, L. O. Chua, *Frequency-domain analysis of nonlinear circuits driven by multi-tone signals*, IEEE Trans. on Circuits and Systems , **31**, *9*, pp. 766-779 (1984).
8. M. Iordache, M. Perpelea, *Modified nodal analysis for large-scale piecewise-linear nonlinear electric circuits*, Rev., Roum., Sci., Techn., - Électrotechn. et Énerg., **37**, *4*, pp. 487-496 (1992).
9. M. Iordache, Lucia Dumitriu, L. Mandache, *Time-Domain Modified Nodal Analysis for Large-Scale Analog Circuits*, Revue Roum. Sci. Techn. - Électrotechn. et Énerg., **48**, *2-3*, pp. 257-268 ( 2003).
10. M. Iordache**,** Lucia Dumitriu**,** *Efficient Decomposition Techniques for Symbolic Analysis of Large – Scale Analog Circuits by State Variable Method*, Analog Circuits and Signal Processing,

Kluwer**, 40**, 3, Kluwer Academic Publishers, pp.235-253 (2004).

11. Angela M. Hodge, R. W. Newcomb, *Semistate Theory and Analog VLSI Design*, IEEE Circuit and Systems Magazine, **2,** *2*, pp.30-49 (2002).

12. L. Mandache, M. Iordache, Lucia Dumitriu, *Time-Domain Modified Nodal Analysis for Analog Circuits*, Proceeding of 7th International Workshop on Symbolic Methods and Applications in Circuit Design, SMACD 2002, October 10-11, Sinaia, Romania, pp. 71-76 (2002).

13. R. Achar, M.S. Nakhla, “Simulation of High-Speed Interconnects”, Proceeding of the IEEE, Vol. 89, No. 5, May 2000, pp. 693-728.